Human Molecular Genetics, 2008, Vol. 17, No. 20 **3223–3235**
doi:10.1093/hmg/ddn218
Advance Access published on July 24, 2008

Blocking acid-sensing ion channel 1 alleviates Huntington's disease pathology via an ubiquitin-proteasome system-dependent mechanism

Hon Kit Wong[1], Peter O. Bauer[1], Masaru Kurosawa[1], Anand Goswami[1], Chika Washizu[1], Yoko Machida[1], Asako Tosaki[1], Mizuki Yamada[1], Thomas Knöpfel[2], Takemichi Nakamura[3] and Nobuyuki Nukina[1,*]

[1]Laboratory for Structural Neuropathology, [2]Laboratory for Neuronal Circuit Dynamics and [3]Biomolecular Characterization, Discovery Research Institute, Molecular Neuropathology Group, RIKEN Brain Science Institute, 2-1 Hirosawa, Wako-shi, Saitama 351-0198, Japan

Received April 22, 2008; Revised June 26, 2008; Accepted July 23, 2008

Huntington's disease (HD) is a fatal neurodegenerative disorder. Despite a tremendous effort to develop therapeutic tools in several HD models, there is no effective cure at present. Acidosis has been observed previously in cellular and in *in vivo* models as well as in the brains of HD patients. Here we challenged HD models with amiloride (Ami) derivative benzamil (Ben), a chemical agent used to rescue acid-sensing ion channel (ASIC)-dependent acidotoxicity, to examine whether chronic acidosis is an important part of the HD pathomechanism and whether these drugs could be used as novel therapeutic agents. Ben markedly reduced the huntingtin-polyglutamine (htt-polyQ) aggregation in an inducible cellular system, and the therapeutic value of Ben was successfully recapitulated in the R6/2 animal model of HD. To reveal the mechanism of action, Ben was found to be able to alleviate the inhibition of the ubiquitin-proteasome system (UPS) activity, resulting in enhanced degradation of soluble htt-polyQ specifically in its pathological range. More importantly, we were able to demonstrate that blocking the expression of a specific isoform of ASIC (*asic1a*), one of the many molecular targets of Ben, led to an enhancement of UPS activity and this blockade also decreased htt-polyQ aggregation in the striatum of R6/2 mice. In conclusion, we believe that chemical compounds that target ASIC1a or pharmacological alleviation of UPS inhibition would be an effective and promising approach to combat HD and other polyQ-related disorders.

INTRODUCTION

Huntington's disease (HD) is still a fatal neurological disorder (1) though it has long been recognized that the CAG repeat expansion (>35–40) in exon 1 of the HD gene (2) causes misfolding of its gene product huntingtin and that results in a toxic gain-of-function. Mutant huntingtin-polyglutamine (htt-polyQ) appears visually as microscopic neuronal intranuclear inclusions well before the onset of symptoms. This strongly implies that htt-polyQ aggregates are required for, or contribute to, the toxicity of HD (3) though recent advances argue that inclusion bodies may play a protective role in HD (4). In any event, as delaying the emergence of visible aggregates in a mouse model of HD ameliorates the severity of disease symptoms, and in many cases extends the survival, the search for chemical compounds that are able to prevent htt-polyQ aggregation has been the focus of extensive research in the last decade (5). Unfortunately, an effective treatment for HD in human patients is still unavailable at the moment.

Diverse theories have been proposed to explain the pathomechanism of HD (6). In particular, numerous lines of evidence from human and animal models strongly support the notion that energy metabolism deficits are likely to be one of the major mechanisms by which HD progresses (7). One of the common and

*To whom correspondence should be addressed. Tel: +81 484679702; Fax: +81 484624796; Email: nukina@brain.riken.jp

widely reported phenomena of energy metabolism impairment in HD is the accumulation of lactate in the central nervous system (CNS) (8–13) and the possible subsequent acidosis (14) in both the human patients and animal models of HD. Although it is unlikely that the level of pH decrease in chronic diseases would be comparable to the acute neurological injuries such as hypoxia and ischemia (15), we asked whether a mild, prolonged and progressive acidification might contribute to the pathogenesis of this neurological disorder. Recent reports suggest that extracellular acidosis is able to activate specific ion channels and that the ablation of these channels offers convincing neuroprotective effect in brain ischemia and other CNS injuries (16,17). Together with the finding that acidosis modulates amyloid beta aggregation (18), we were inspired to investigate the role of acid-sensing ion channels (ASICs) in the pathogenesis of HD.

The ASICs belong to the H^+-gated subgroup of the mammalian degenerin/epithelial sodium channel (DEG/ENaC) superfamily. They are cation selective (19) and are predominantly expressed in the nervous system (20). Six subunits of ASICs have been identified so far (21) and among which 1b and 3 are mainly expressed in the peripheral nervous system (PNS). ASIC isoforms 3 and 4 may play essential roles in the PNS as nociceptors and mechanoreceptors (22). On the other hand, ASIC1 and 2 isoforms are widely and ubiquitously distributed in the CNS and particularly enriched in areas that are most susceptible to htt-polyQ-mediated protein aggregation and degeneration such as cingulate cortex and striatum (23). This area-specific enrichment of ASICs perhaps highlights the potential participation of these channel proteins in mediating HD pathogenesis. Loss of ASIC1a disrupted hippocampal-dependent long-term potentiation (LTP), spatial memory in the Morris water maze and cerebellum-dependent learning (24) suggest that ASIC1a modulates synaptic plasticity and contributes to learning and memory under physiological conditions. In addition, as ASICs composed of ASIC1a subunit are activated by extracellular protons and permeable to calcium ions (19,25), ASICs are equally and importantly anticipated to be involved in pathological conditions such as pain (26,27) and ischemic stroke (16,28).

Amiloride (Ami) is a pyrazinoylguanidine bearing amino groups in the 3′ and 5′ positions and a chloro group in the 6-position of the pyrazine ring. It was synthesized in the mid-1960s while in search of diuretic agents that possessed both natriuretic and antikaliuretic properties (29), and has been used in clinics as an adjunctive treatment in congestive heart failure or hypertension. Ami is widely used as a specific blocker of ASIC and targets also several other protein exchangers such as sodium/hydrogen exchanger (NHE) and sodium/calcium exchanger (NCX) (30). By substituting benzyl on the terminal hydrogen atom of the guanidino moiety, benzamil (Ben) has been produced as one of the more specific inhibitors of epithelial sodium channels (31). Ami attenuated acidosis-induced cellular damage (17) and intracerebroventricular injection of Ami protects the CNS from ischemic injury (16). These recent studies undoubtedly highlight the use of Ami and perhaps its analogs as neuroprotective drugs in acidosis-mediated brain injuries.

Assuming that chronic tissue acidosis might be indeed one of the unknown underlying pathomechanisms of HD, here we assessed the therapeutic values of Ami and Ben using cellular and animal models of HD and delineated the molecular mechanism by which they ameliorate HD pathological processes. Ben markedly reduced the polyQ aggregation and toxicity in both the *in vitro* and *in vivo* models, and importantly, the underlying mechanism was proven to be ubiquitin-proteasome system (UPS) and ASIC1a-dependent.

RESULTS

Ami and Ben reduces Nhtt-polyQ aggregation in a dose-dependent manner

The progressively acidification of cell culture medium derived from primary post-natal cerebrocortical neurons expressing htt-polyQ-EGFP (32) provided the first evidence that the acid-base balance in HD is distributed (Supplementary Material, Fig. S1A). Further examination of the intracellular pH (pH_i) in a well-characterized stable mouse Neuro2a cell system (33) revealed that the cells that had been induced to form N-terminal huntingtin (Nhtt)-150Q-EGFP had a significant lower pH_i compared with the non-induced control. Assuming that this state leads to the pH-sensitive ASIC opening (34), co-incubation with a highly specific ASIC blocker Ben was indeed able to restore the pH_i back to the control levels (Supplementary Material, Fig. S1B), suggesting the involvement of ASICs in HD pathogenesis.

To test further whether blocking ASICs by Ami and Ben might provide additional beneficial effects in models of HD, first we focused on their effect on htt-polyQ aggregation. We found that Ami and Ben decreased truncated Nhtt exon 1-60Q-EGFP and Nhtt-150Q-EGFP cytoplasmic aggregates markedly in a dose-dependent manner (Fig. 1A) without significant toxicity up to 50 μM (Fig. 1B). These compounds also reduced Nhtt-150Qnls-EGFP nuclear aggregates significantly in the same inducible system (Fig. 1C) and both the cytoplasmic and nuclear aggregates in a transient transfection system with various lengths of polyQ repeats (Fig. 1D; Ami, data not shown). Filter trap assay (FTA) also showed that Ami and Ben reduced the SDS-insoluble aggregates that were trapped on top of the cellulose acetate membrane (Fig. 1E). As semi-quantitative PCR showed that these chemicals did not affect the expression of Nhtt-16/60/150Q-EGFP (Fig. 1F), these data suggest that these drugs reduce the Nhtt-polyQ aggregation via a post-transcriptional mechanism.

Ben ameliorates HD pathology in R6/2 mice

We further assessed the effect of Ami derivatives in the HD mouse model R6/2 so as to confirm its therapeutic value *in vivo*. We prefer Ben to Ami for our mouse studies because the greater hydrophobicity of Ben (30) may assist delivery. We prepared whole brain lysates from wild type, and transgenic (tg) R6/2 mice either untreated, or treated with various concentrations of Ben and analyzed the SDS-insoluble htt-polyQ aggregation by FTA. As shown in Fig. 2A, a significant decrease of aggregation was observed in the mice that were treated with Ben1 (1 mg/kg) or Ben5 (5 mg/kg), there being a >30% reduction detected by the anti-htt (em48) antibody at both 8 and 12 weeks of age (Fig. 2B). Quantifying the amount of ubiquitin-positive aggregates in the cingulate area 1/2 (Cg1/Cg2) of the cerebral cortex from these mice also

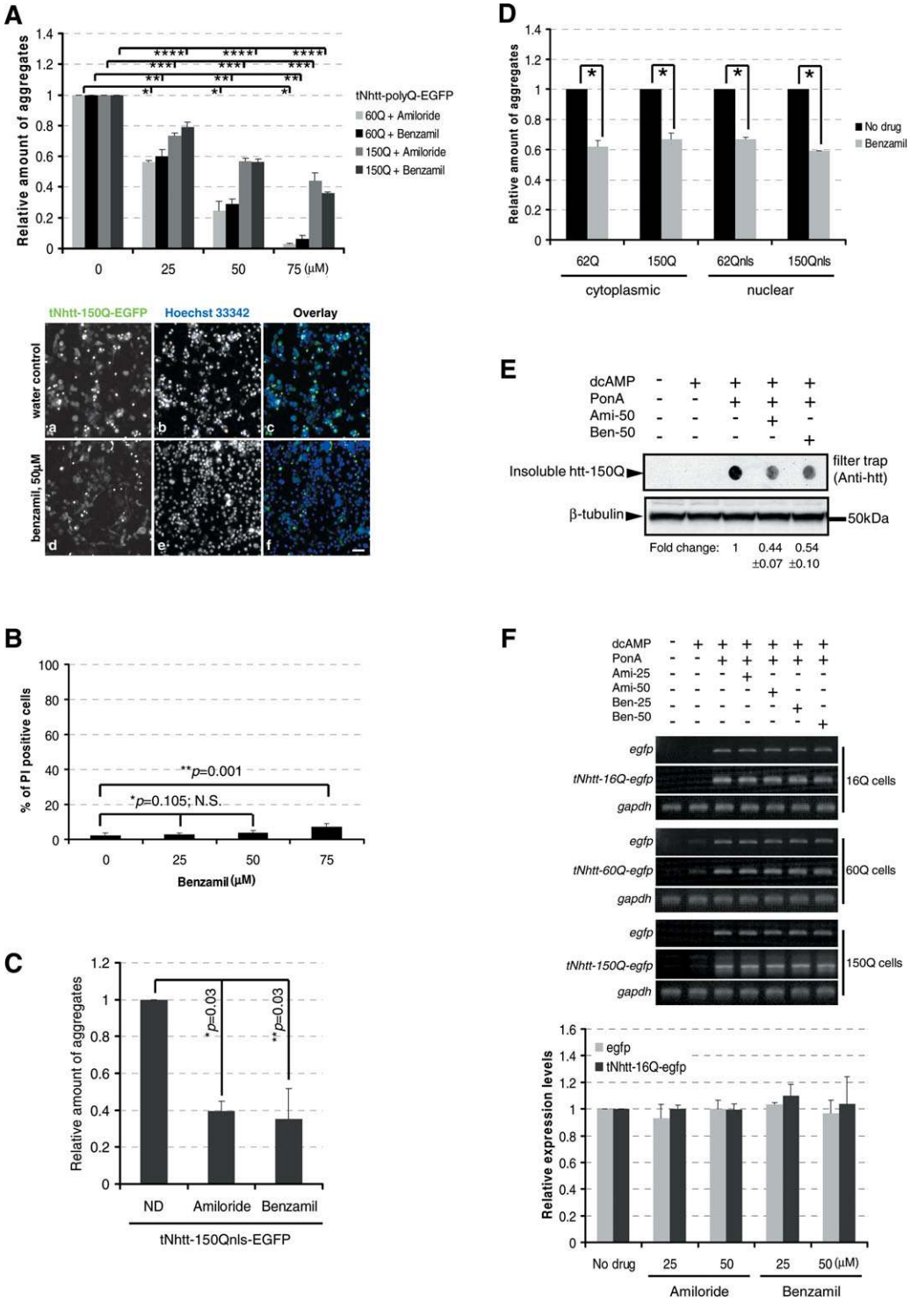

Figure 1. Ami and Ben reduce Nhtt-polyQ aggregation in a dose-dependent manner via a post-transcriptional mechanism. (**A**) Ami or Ben reduces Nhtt-polyQ aggregation in a dose-dependent manner. The reduction of Nhtt-150Q-EGFP aggregation by Ben was shown visually in the lower panel (d–f). $n = 5$, * and $^{**}P = 0.019$; *** and $^{****}P < 0.0001$, comparison between treated and non-treated. Scale bar = 80 μm. (**B**) Addition of Ben up to 50 μM does not cause significant toxicity to Neuro2a cells. Neuro2a cells that were treated with various concentrations of Ben for 24 h as indicated were subsequently stained with 5 μg/ml proprium iodide (PI). The number of PI-positive cells were quantified with ArrayScan. $n = 3$, $^{*}P = 0.105$; $^{**}P = 0.001$. N.S., not significant. (**C**) Ami or Ben at 50 μM reduces Nhtt-150Qnls-EGFP nuclear aggregates, quantified by ArrayScan. $n = 3$, * and $^{**}P = 0.03$. ND, no drug. (**D**) Ben reduces the amount of aggregates formed by Nhtt-polyQ ($^{+/-}$ nls) in a transient expression system. The number of EGFP-positive aggregates was counted 12 h after transfection with ArrayScan. $n = 3$, $^{*}P < 0.0001$. nls, nuclear localization signal. (**E**) A FTA illustrates the reduction of aggregates by Ami and Ben. $n = 4$, fold change shows mean ± SEM. (**F**) Semi-quantitative PCR shows virtually unaltered expression of Nhtt-polyQ-EGFP in cells that were treated with various concentrations of Ami and Ben. Expression levels of the transgene were amplified with primers targeting either EGFP or Nhtt-polyQ-EGFP. Gapdh shows equal cDNA input. Quantification of the PCR results for that of Nhtt-16Q-EGFP is shown in the lower panel. $n = 3$.

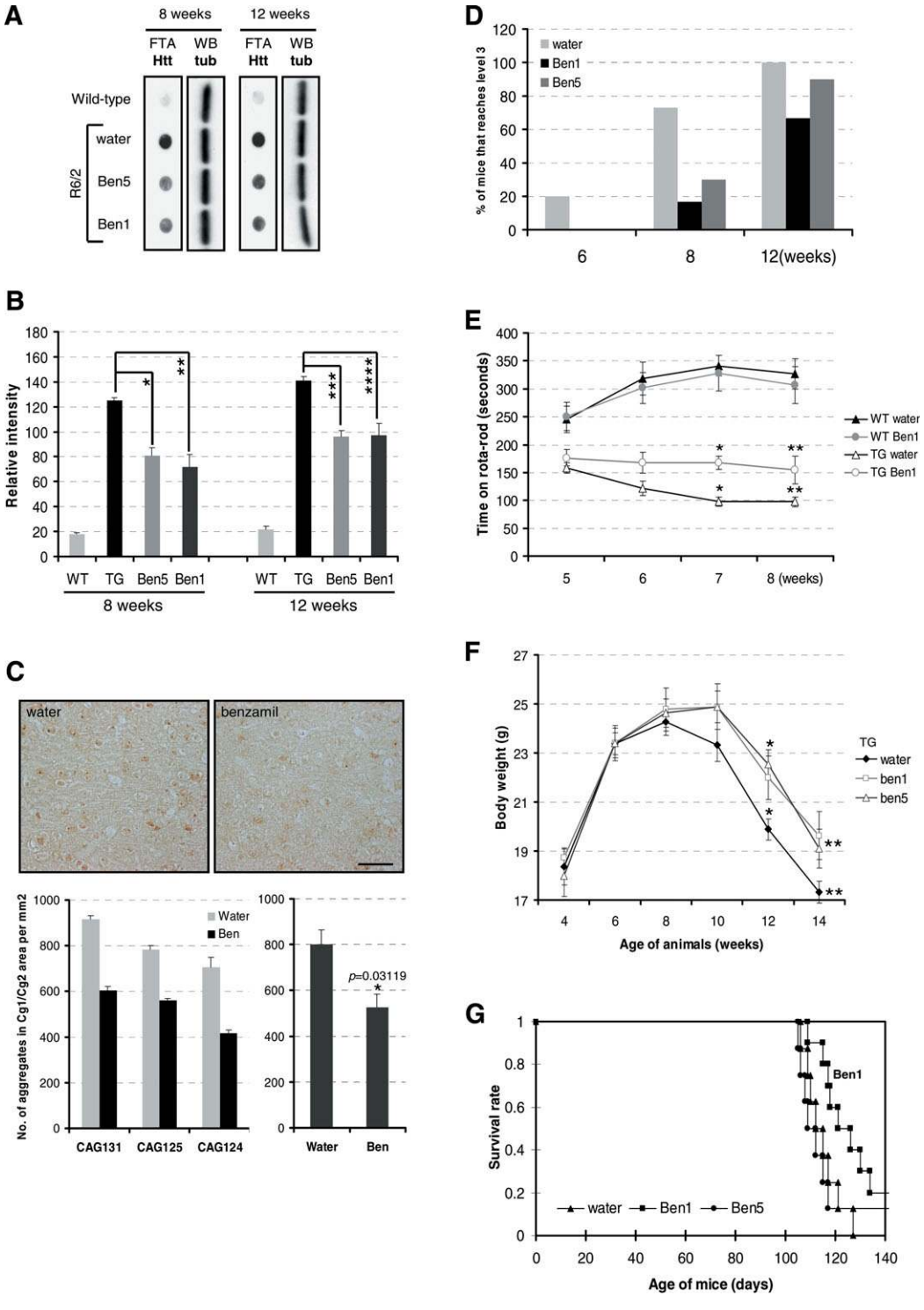

Figure 2. Ben ameliorates brain pathology, motor deficits and increases life span of R6/2 mice. (**A** and **B**) Ben reduces the amount of SDS-resistant aggregates in the brain of R6/2 mice. (A) Shows the SDS insoluble aggregates on a cellulose acetate membrane (β-tubulin shows the equal amount of protein in each sample) and (B) shows the quantification results from the average of three animals in each treatment. $^{*}P = 0.009$; $^{**}P = 0.004$; *** and $^{****}P = 0.007$. (**C**) Ben reduces the number of visible, ubiquitin-positive aggregates in the cerebral cortex (Cg1/Cg2 area) of R6/2 mice. Upper panels show the immunohistochemical micrographs and lower panels show the quantification of visible aggregates in the Cg1/Cg2 area of the cerebral cortex of R6/2 at 8 weeks of age carrying different length of polyQ repeats. The number of aggregates was normalized to the area of each micrograph that corresponded to 0.325 mm^2 of the brain section. Scale bar = 0.02 mm, $^{*}P = 0.03119$. (**D**) Clasping score. Ben treatment markedly reduces the number of mice reaching clasping score level 3 at both 8 weeks and 12 weeks. Tg-water, $n = 11$; tg-Ben1, $n = 13$, tg-Ben5, $n = 10$. (**E**) Rota-rod test. Ben of 1 mg/kg alleviates the motor deficit of R6/2 mice by decreasing their latency to fall on rotating rod at and after 7 weeks of age. $n = 5$ in each group. $^{*}P = 0.0015$ and $^{**}P = 0.042$. (**F**) Ben treatment increases body weight of R6/2 mice. Tg-water, $n = 11$; tg-Ben1, $n = 13$, tg-Ben5, $n = 10$. $^{*}P = 0.034$ and $^{**}P = 0.044$. (**G**) Ben significantly extends the lifespan of R6/2 mice. Survival data from each treatment was analyzed by Kaplan–Meier method followed by log-rank testing. Tg-water, $n = 9$; tg-Ben1, $n = 11$ and tg-Ben5, $n = 10$.

revealed a >30% reduction of aggregation in mice carrying various length of polyQ repeats (Fig. 2C). Accompanied by the amelioration of brain pathology, the limb clasping posture of R6/2 mice was also significantly ameliorated in the mice that were being fed with Ben at both 8 and 12 weeks of age (Fig. 2D). Rota-rod studies further showed that Ben greatly reduced the latency to fall on rota-rod from 7 weeks of age, suggesting that the motor impairment of R6/2 was indeed reduced (Fig. 2E). The beneficial effect of Ben was also revealed by a significant increase of body weight after 10 weeks of age (Fig. 2F). More importantly, Ben1 significantly increased the survival of R6/2 mice (Fig. 2G). The mean survival time for tg-water is 114.625 ± 2.44 days while that of tg-Ben1 is 126.1 ± 4.001 days (tg-water versus tg-Ben1, $P = 0.024$). As both Ben5 and Ben1 decreased aggregation in the R6/2 mouse brain but only Ben1 significantly increased the survival rate, it has to be noted that the potential side effects of Ben could outweigh its beneficial effect at high concentrations in this disease model. Indeed, Ben10 also reduced the htt-polyQ aggregation in the R6/2 mouse brain but decreased the survival rate compared with that of wild type (data not shown). Collectively, data obtained from both the cellular and animal models of HD strongly suggest that Ben is a novel drug therapy for HD.

Ben induce a polyQ length-dependent degradation of soluble mutant huntingtin

After we were convinced that Ben is able to reduce HD aggregation both *in vitro* and *in vivo*, we focused on investigating the molecular mechanism(s) by which Ben works for the rest of the studies. Given that Ben do not affect the expression of Nhtt-polyQ at the transcriptional level (Fig. 1F), the significant and prominent decrease on the soluble form of mutant htt in the presence of Ben (Fig. 3A and B) prompted us to reason that Ben may reduce aggregation by working through the protein degradation system.

For this purpose, we did a chase experiment to examine whether Ben would affect the degradation of soluble mutant htt protein. We used Nhtt-60Q in this experiment because majority of the Nhtt-60Q stayed soluble after induction. As illustrated in the left panel of Fig. 3C, Ben markedly enhanced the initial degradation of Nhtt-60Q and there was a significant decrease in the absolute amount of soluble mutant Nhtt-60Q in the presence of Ben at Day 3 and Day 4. The half-life of soluble Nhtt-60Q was determined to be 3.846 ± 0.32 and 2.721 ± 0.52 days for water and Ben, respectively. The same experiment for Nhtt-16Q was also performed and it appeared that there was no significant difference in the absolute amount of 16Q protein after the addition of Ben (Fig. 3C, right). These results clearly demonstrate that Ben enhances the degradation of soluble Nhtt-polyQ specifically in its pathological range.

Ben alleviates UPS inhibition *in vivo*

To investigate which degradation system is modulated by Ben, first we examined the UPS activity with an expression construct that encodes a ubiquitin (ubi) tagged Discosoma Red fluorescent protein (ubi-dsRED) (35), with monomeric red

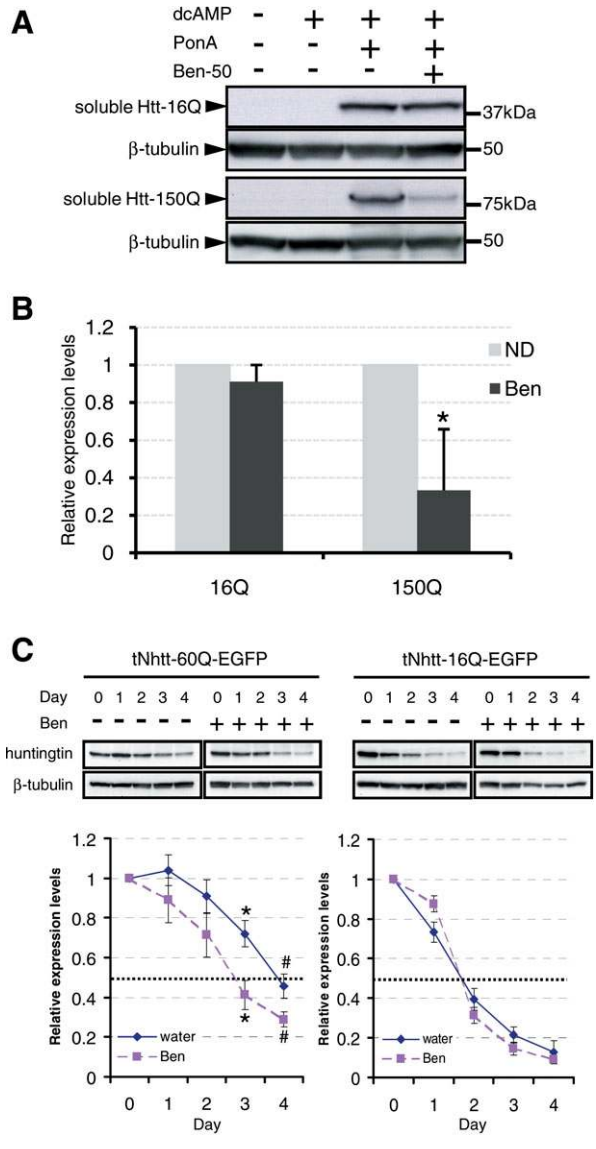

Figure 3. Ben induces a polyQ length-dependent degradation of soluble mutant huntingtin. (**A** and **B**) Ben treatment leads to a decreased expression of soluble mutant htt-polyQ at the protein level. There was a 40–50% decrease of soluble Nhtt-150Q expression 1 day after treatment with Ben at 50 μM, while that of Nhtt-16Q remained virtually unchanged. $n = 3$, $^{*}P < 0.001$. (**C**) Ben enhances the degradation of soluble mutant Nhtt-60Q-EGFP. Neuro2a cells were induced to express Nhtt-60Q-EGFP for 1 day, and the inducer was removed and Ben was added. The addition of Ben enhanced the degradation of soluble Nhtt-60Q-EGFP while that of Nhtt-16Q-EGFP was not significantly altered. The absolute amount of 60Q protein was significantly reduced 3 and 4 days after the addition of Ben as revealed by the anti-htt antibodies. $n = 3$, $^{*}P = 0.037$ and $^{\#}P = 0.039$.

fluorescence protein (mRFP) as a control (36). Ben dose-dependently reduced the accumulation of ubi-dsRED caused by low concentrations of MG-132 suggesting that Ben is capable of alleviating the global UPS inhibition caused by a reversible proteasome inhibitor (Supplementary Material, Fig. S2A). Next we examined whether Ben could also alleviate the UPS inhibition caused by mutant Nhtt-polyQ aggregation, knowing that the UPS activity was blocked in a polyQ length-dependent manner (Supplementary Material, Fig. S2B).

Ben reduced the co-expression of ubi-dsRED and htt-62Q aggregates (Fig. 4Ac–f and B, Ubi-dsRED) and had virtually no effect on that of mRFP and htt-62Q aggregates (Fig. 4Aa and B, RFP). Consequently, the number of ubi-dsRED-positive cells (Fig. 4C) and the average ubi-dsRED intensity (data not shown) in aggregate-containing cells was also reduced. Western blotting with anti-RFP antibodies with these cell lysates recapitulated faithfully the ArrayScan results (Fig. 4D). Essentially the same results were obtained with the proteasome sensor vector containing a destabilized GFP (ZsGreen) (Supplementary Material, Fig. S3). These data suggest that Ben alleviated the UPS blockade caused by mutant Nhtt-polyQ.

To further clarify the degradation pathway(s) by which Ben acts, we blocked the function of the UPS with specific proteasome inhibitors and examined whether Ben could still reduce Nhtt-polyQ aggregation. Consistent with the notion that Ben reduces polyQ aggregation by alleviating the UPS inhibition, further blockade of the UPS by treatment with either lactacystin or MG-132 significantly and largely attenuated the effect of Ben (Fig. 4E). Probing the lysates prepared from the cells treated with proteasome inhibitors with anti-ubiquitin antibodies revealed that proteasome inhibitors could completely antagonize the effect of Ben in reducing the amount of poly-ubiquitinated proteins, further suggesting that these drugs reduce aggregation dominantly by employing the UPS (Fig. 4F). The presence or absence of Atg5 did not affect the function of Ben suggesting that macroautophagy was not required for the clearance of mutant Nhtt-polyQ in this treatment (Supplementary Material, Fig. S4).

For a final examination to investigate whether Ben increases UPS activity in the intact mammalian brain, we generated a mouse line in which the expression of an unstable version of EGFP (d2EGFP) (37) is driven by 5′ regulatory sequences of the voltage-gated potassium channel gene KCNC3 (38). Controls to demonstrate this mouse line as a valid tool to reflect brain UPS activity are shown in Supplementary Material, Fig. S5. We fed either water or Ben to the d2EGFP mice from 4 weeks of age and sacrificed them at 8 weeks for d2EGFP-DAB immunohistochemistry to reveal the general UPS activity in the brain. Oral feeding with water produced around 80 DAB-positive d2EGFP cells per millimeter square, probably due to the overexpression of d2EGFP at high levels in certain population of cells, and Ben reduced the number down to around 50 (Fig. 4G), suggesting an enhancement of UPS activity. Taken all together, both the *in vitro* and *in vivo* data generated with various kinds of degron constructs strongly and unambiguously support the notion that Ben enhances the general UPS activity in neurons and in the mammalian CNS.

Suppressing the expression of *asic1a* enhances UPS activity and reduces Nhtt-polyQ aggregation

Having shown that Ben reduced Nhtt-polyQ aggregation by alleviating the UPS inhibition, we further investigated the underlying mechanism and searched the molecular target(s) by which UPS is modulated. We made short hairpin (sh) RNA for some of the major molecular targets of Ami and derivatives to try to mimic the pharmacological blockade of these channel proteins by Ben. Supplementary Material, Fig. S6 shows the knockdown efficiency at the transcriptional levels (A), translational levels (B) and the specificity of these shRNAs (C and D). Suppressing the expression of *asic*s and/or *ncx*s led to a significant reduction of ubi-dsRED cells while that of RFP was unchanged (Fig. 5A). More, inhibiting the expression of *asic* (either *1a* or *2a*, Fig. 5B) or *ncx* (only *ncx2* and *ncx3*, Fig. 5C) reduced the percentage of aggregation significantly by 30–40%. Blocking all the variants of *asic* and *ncx* together further decreased the amount of aggregates in both 60Q and 150Q cells (Fig. 5D). Interestingly, blocking either *nhe1* or *nhe5* or both variants did not lead to a significant reduction of ubi-dsRED cells or htt-polyQ aggregation (data not shown), suggesting that channels that are normally used for regulating physiological pH do not involve in HD pathogenesis. These data confirm our initial idea and hypothesis that ASICs are indeed the major molecules targeted by Ami and its derivatives.

We further explored the role of these channel proteins in HD pathomechanism in the mammalian brain. We decided to examine only the role of *asic1a* in HD pathogenesis because there was a significant decrease of *ncx2* and *ncx3* expression in the R6/2 mouse at and after 8 weeks of age (Supplementary Material, Fig. S7). To achieve maximum knockdown of *asic1a* in the mouse brain, we cloned *asic1a* microRNA (miR) into pcDNA6.2^{TM}-GW/RFP-miR in which the expression can be driven by a CMV promoter and be keeping track with RFP. Using these RNAi constructs we achieved a >70–80% knockdown of endogenous *asic1a* in neuro2a cells (Fig. 5E, upper). These constructs were further subcloned into rAVE^{TM} cassettes (GeneDetect) and packaged into chimeric recombinant adeno-associated viruses genotype 1/2 (rAAV1/2) to maximize the infection efficiency in mouse brain tissues (39). Stereotaxic injection of these viruses into mouse striatum showed similar infection efficiency (Fig. 5E, lower). Suppressing the expression of *asic1a* in the mouse striatum was able to reduce htt-polyQ aggregation and on average there being a 60% reduction of aggregation revealed by anti-htt antibodies (Fig. 5F). Taken all the data together, we strongly believe that Ben blocks *asic1a*, resulting in a global enhancement of UPS activity and that possibly explains the underlying mechanism by which Ben alleviates the pathological processes of HD.

DISCUSSION

In this article, we report Ben as a novel drug candidate in the treatment of HD and clearly demonstrated that this compound reduces mutant htt-polyQ aggregation by alleviating UPS inhibition in several models of HD. We also identified *asic1a* as the possible therapeutic target for the reduction of htt-polyQ aggregation. Our studies strongly suggest that alleviating the UPS inhibition or enhancing the UPS in a controlled manner would be an attractive and promising strategy to combat HD, and possibly other neurodegenerative disorders. This is the second report demonstrating that ASICs play an important role in chronic neurological diseases (40) and the first in polyQ-mediated neurodegeneration.

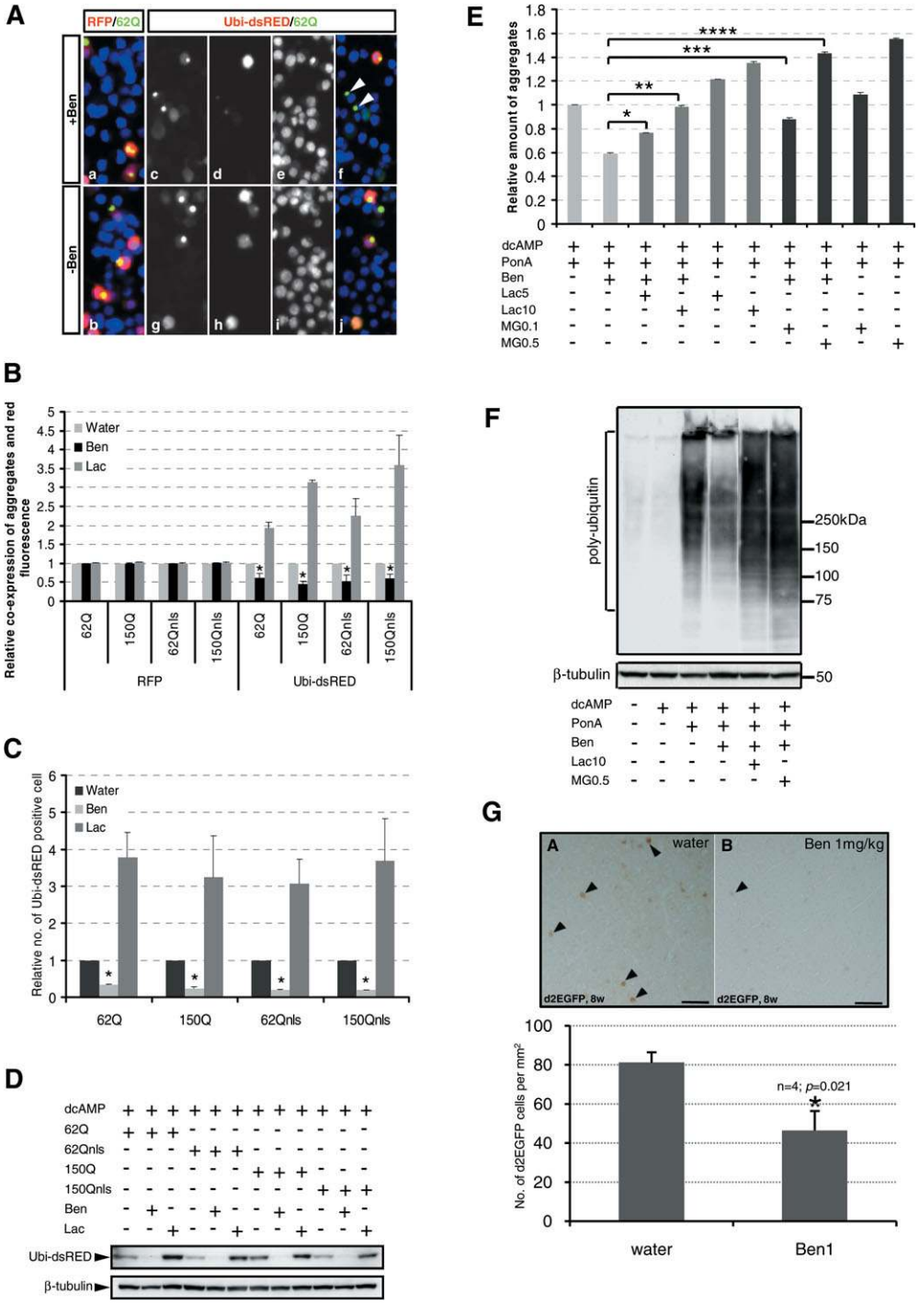

Figure 4. Ben alleviates the inhibition of UPS *in vivo*. (**A**–**D**) Ben attenuates the blockade of UPS caused by mutant Nhtt-polyQ. Fluorescence micrographs showing the effect of Ben on the co-expression of RFP or ubi-dsRED and Nhtt-62Q aggregates (A). The addition of Ben reduced the accumulation of ubi-dsRED in cells that contain aggregates (Ac–f, arrowheads and B, Ubi-dsRED) while that of RFP (Aa and B, RFP) was virtually unaltered. ArrayScan counting also revealed that the number of ubi-dsRED-positive cells (C) was reduced in the presence of Ben. Furthermore, the reduced accumulation of ubi-dsRED was shown by a western blot that analyzed with anti-RFP antibodies (D). Lactacystin (10 μM) was used as a positive control for the inhibition of UPS. $n = 3$, $^{*}P < 0.0001$ compared with the water control. (**E**) Blocking the UPS markedly abolishes the effect of Ben. On top of ponasterone A induction of Nhtt-150Q, Neuro2a cells were incubated with Ben and proteasome inhibitor lactacystin or MG-132, at two different concentrations (in μM). Lactacystin or MG-132 markedly abolished the effect of Ben suggesting that the UPS was the degradation system primarily employed by Ben for Nhtt-polyQ clearance. $n = 3$, $^{*}P = 0.006$; **, *** and $^{****}P < 0.0001$. (**F**) Western blotting analysis with anti-ubiquitin antibodies also revealed that proteasome inhibition was enough to abolish the effect of Ben. Ben reduced the amount of ubiquitinated proteins in the presence of Nhtt-150Q, while the co-incubation with proteasome inhibitors abolished this effect. Beta-tubulin shows equal protein loading. $n = 3$. (**G**) Ben increases brain UPS activity. Feeding d2EGFP mice with 1 mg/kg Ben for 4 weeks reduced the number of d2EGFP cells in the somatosensory cortex (A and B; arrowheads, d2EGFP cells; scale bar = 50 μm). Lower panel shows the quantification (number per mm^2). $n = 4$; $P = 0.021$.

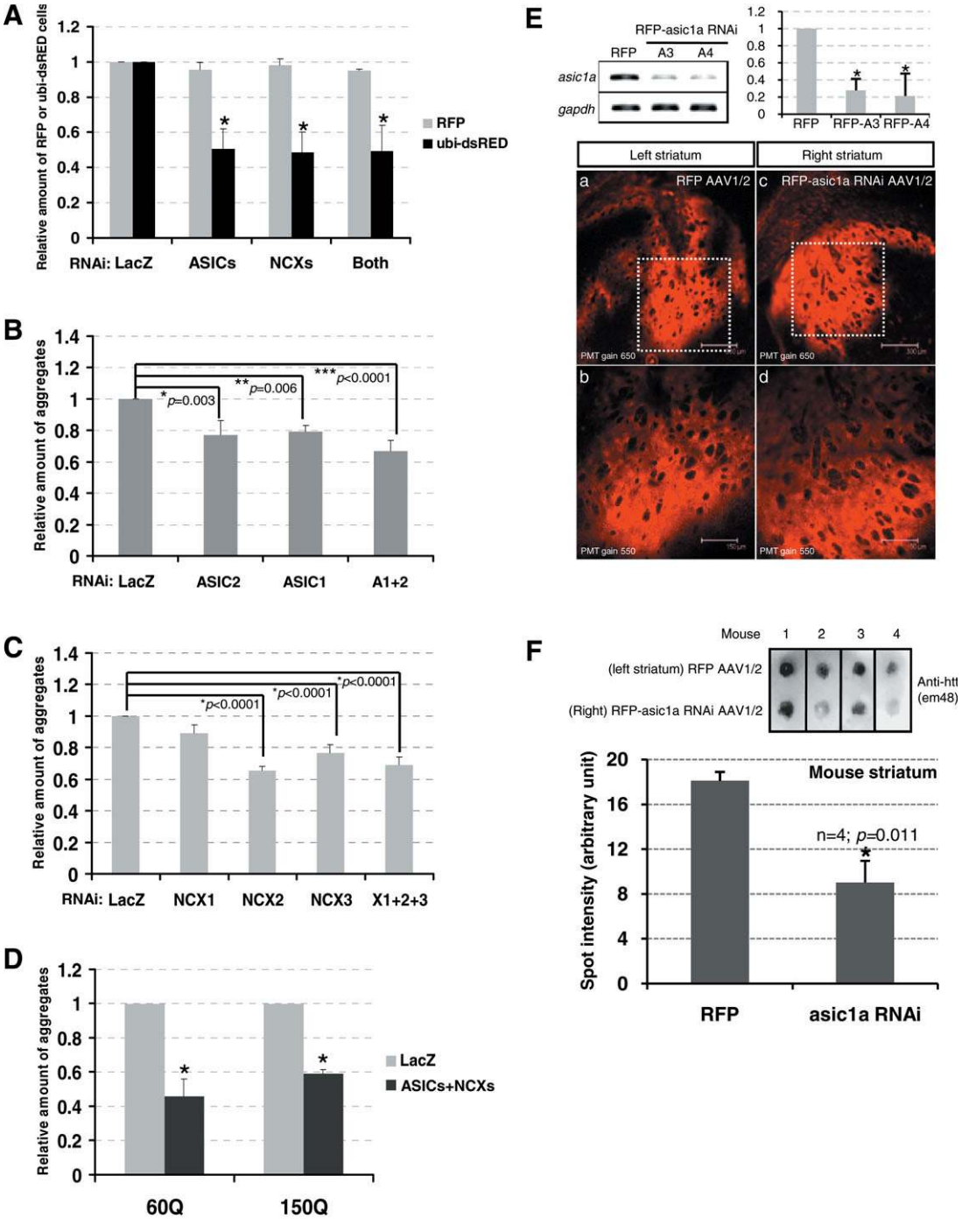

Figure 5. Silencing the expression of *asic1a* reduces Nhtt-polyQ aggregation *in vivo*. (**A**) Silencing the expression of *asic*s, *ncx*s or both leads to a significant increase of UPS activity. Neuro2a cells were first transfected with the corresponding shRNAs for 2 days to allow gene silencing. Seventy nanogram of RFP or ubi-dsRED construct was subsequently transfected for the determination of UPS activity. The number of RFP or ubi-dsRED cells was quantified by ArrayScan. The number of RFP or ubi-dsRED cells in the LacZ RNAi-transfected condition was set at 1 and the others were compared to this control accordingly. While there was no significant change of the number of RFP cells, that of ubi-dsRED was markedly decreased when the expression of *asic*s and/or *ncx*s was blocked. $n = 3$, $^{*}P < 0.0001$ compared with the LacZ control. (**B**) Silencing the expression of *asic1a* or *asic2a* reduces the aggregation of Nhtt-150Q. $n = 9$, $^{*}P = 0.03$; $^{**}P = 0.006$ and $^{***}P < 0.0001$. (**C**) Silencing the expression of *ncx2* or *ncx3* reduces the aggregation of Nhtt-150Q. $n = 9$, $^{*}P < 0.0001$. (**D**) Silencing the expression of both the *asic*s and *ncx*s reduces the aggregation of Nhtt-60Q and Nhtt-150Q. $n = 5$, $^{*}P < 0.0001$. (**E**) The knockdown efficiency of *asic1a* miR RNAi (upper) and the infection efficiency of AAV1/2 in the mouse striatum (lower). (b and d) Are the magnified images of (a and c), respectively. RFP and RFP-*asic1a* RNAi show comparable infection efficiency both intensity and anatomy-wise. Scale bars in (a and c) = 300 μm and (b and d) = 150 μm; PMT represents photo multiplier tubes. (**F**) Suppressing the expression of *asic1a* reduces htt-polyQ aggregation in R6/2 mice. AAV1/2 encoding RFP or RFP-*asic1a* RNAi was stereostaxically injected into the striatum of R6/2 mice at 4 weeks of age and the striatal area was collected for filter trap analysis at 8 weeks of age. Inhibition of *asic1a* expression reduces htt-polyQ aggregation as revealed by anti-htt antibodies. Quantifying the spots intensity on filter trap shows a 60% of reduction of polyQ aggregation, normalized to β-tubulin. $n = 4$, $P = 0.0048$.

We tested the therapeutic value of Ami derivative assuming that acidosis contribute to one of the underlying pathomechanisms of HD and found that blocking ASICs alleviates the UPS inhibition and the subsequent aggregate load. Though we do not have direct experimental data showing that ASIC1a is indeed activated during pH fluctuations and the precise mechanism(s) by which ASIC1a connects to the modulation of UPS remains to be established, we provided unambiguous evidence that blocking the activity and/or expression of ASIC1a, with either Ben or ASIC1a RNA interference, leads to an overall beneficial effect in cellular and animal models of HD. These results support the notion that acidosis and the subsequent activation of ASIC1a plays a role in the polyQ aggregating process and the pathogenesis of HD. As one of the major physiological and perhaps pathological consequences of ASIC1a activation concerns calcium influx (17), it may well be that blocking ASIC1a reduces calcium influx and eventually limits the rate of aggregate formation. Indeed, preliminary results show that calmodulin inhibitors w-5 and w-7 potently reduce the htt-polyQ formation *in vitro* (unpublished data).

Another interesting discovery in this study is that UPS activity can also be elevated by blocking another molecular target of Ben, the NCX. To the best of our knowledge, the direct and precise connection between NCX and the UPS activity has not been established. The major physiological function of NCX is to exclude Ca^{2+} from the cytosol to orchestrate normal cellular Ca^{2+} homeostasis in a variety of tissues. However, under certain pathological conditions like global brain ischemia, when cytosolic $[Na^{+}]$ increases and plasma membrane potential depolarizes, the equilibrium potential of NCX may become more negative than the plasma membrane potential, causing the reversal of the exchanger (41). Assuming that HD pathogenesis is mediated by chronic acidosis and the elevation of cytosolic $[Ca^{2+}]$ is partly through NCX working in the reverse mode, blocking NCX and reducing the calcium influx may lead to a better function of the 11S regulatory (REG)/proteasome activator 28 (PA28) (42) though it has to be noted that recent studies indicate that calcium could do otherwise (43,44). Perhaps the role of calcium in regulating UPS activity is highly system and time-dependent. As the expression of NCX mRNA levels declines when the disease progresses (Supplementary Material, Fig. S7), though the precise mechanism by which NCX works in the cellular systems is interesting to be pursued, we believe that blocking the expression and/or function of this exchanger may not be a promising therapeutic target in treating HD.

While the role of calcium ions and calcium signal transduction proteins in our experimental scenario remains to be further explored, we are able to show that UPS activity is enhanced with Ben or inhibition of ASIC1a using various degron constructs. It raised an interesting hypothesis that the UPS activity can be modulated with changes in either extracellular or pH_i. Indeed, this idea is supported by a report showing that pH rise at fertilization is a necessary prerequisite for activation of proteasome (45). As the UPS activity has also been reported to be impaired after transient forebrain ischemia (46) and during the ischemia-reperfusion period (47), it may well be that the neuroprotective effect offered by Ami and derivatives may also be connected to the pH or ASIC1a-mediated alleviation of UPS impairment. If the causal relationship between UPS activity and pH_i can be proven directly, the enhancement of UPS activity by modulating pH_i could be considered as a novel strategy to combat acidosis-mediated neurological disorders.

The degradation of misfolded and damaged proteins by the UPS is essential to maintain protein quality control, and the aberrant functioning of the UPS has been linked to a number of human disorders (48), including neurodegenerative diseases such as Parkinson's disease (49). In fact, the impaired UPS function caused by expanded polyQ was well established by our group and the others in various *in vitro* and *in vivo* models of HD (35,50–52). Very recently, the global inhibition of UPS has been confirmed in the mammalian brain with two different HD mouse models, perhaps enough to demonstrate the importance of UPS disturbances as one of the major causes (or consequences) of polyQ-initiated neurodegeneration (53). The data produced with Ben support the notion that impairment of UPS is indeed one of the core pathomechanisms of HD, and further extend the idea that alleviation of UPS inhibition can reduce htt-polyQ aggregation and ameliorates the pathological processes in R6/2 mice. To the best of our knowledge, Ben is the first chemical compound that is capable of enhancing UPS activity in a concentration-dependent manner. The fact that Ben also shows beneficial effects in lung (54) and cardiac (55) disease models extends its potential use as a drug in human. Ami, on the other hand, has already been prescribed as an adjunctive treatment with thiazide diuretics or other kaliuretic agents in congestive heart failure or hypertension (56) in human patients with known pharmacokinetics. Whether there are patients of HD or other neurodegenerative diseases being prescribed with Ami due to hypertension should be explored, and the clinical course of those patients should be carefully examined so that the true therapeutic value of Ami can be better understood.

It has been reported that there are more than 1000 analogs of Ami (57) and novel blockers of Ami has been developing (58). Therefore, it is highly likely that a non-toxic derivative(s) that is even more effective than Ben can be discovered in the near future. This class of drugs may thus open a new avenue for combating HD and potentially to other neurodegenerative diseases with similar pathomechanisms.

MATERIALS AND METHODS

Reagents and antibodies

Amiloride.HCl and Benzamil.HCl were from Alexis or Sigma; Lactacystin was from Peptide Institute; MG-132 (Z-Leu-Leu-Leu-aldehyde) was from Wako Chemicals; anti-ATG5 antibodies was kindly provided by Dr Mizushima (59); anti-huntingtin antibodies (MAB5374) and anti-β-tubulin antibodies (MAB3408) were from Chemicon; anti-LC3 (PD014), anti-GFP (598) and anti-RFP (PM005) antibodies were from MBL; anti-ubiquitin antibodies (Z0458) was from DAKO; anti-V5 antibodies was from Invitrogen. All other chemicals were from Sigma or Nacalai tesque unless otherwise specified.

Expression constructs

Plasmids encoding the truncated N-terminal of human huntingtin with either 17, 62 or 150 glutamine repeats fused to enhanced GFP were introduced in pEGFP-N1 vector as previously described (33). The mRFP (36) and the ubi-dsRed2/N1 plasmids (35) were previously described. The proteasome sensor vector was from Clontech. We cloned full-length channel or exchanger into pcDNA^{TM}3.1/V5-His TOPO® TA expression vector (Invitrogen) according to the instruction manual. Full-length mRNA sequence of each gene was amplified with a nested PCR strategy. Accession No. for each mRNA is shown as follow: NHE-1, U51112; NHE-5, AF111173; NCX-1, NM_011406; NCX-2, NM_148946; NCX-3, NM_080440; BNaC1, BC038551; BNaC2, NM_009597. All plasmids were sequence-verified and their expression and expected molecular weight was checked with anti-V5 antibodies (Invitrogen) on western blots.

Generation and stereotaxic injection of AAV1/2 encoding RFP or RFP-asic1a miR RNAi into R6/2 mouse brain

miR RNAi against *asic1a* (all 5′ to 3′; A3, gcccttcaacatgcgtgagtt; A4, ggtatgggaagtgctacacat) was first cloned into pcDNA6.2^{TM}-GW/RFP-miR (The BLOCK-iT^{TM} Pol II miR RNAi Expression Vector Kits from Invitrogen) and further subcloned into rAVE^{TM} cassette that is flanked by the AAV inverted terminal repeats (ITR). The transgene is driven by the hybrid chicken β-actin/CMV enhancer (CAG) promoter and enhanced expression is achieved by the addition of regulatory elements scaffold-attachment region (SAR) and woodchuck post-regulatory regulatory element (WPRE). These constructs were then packaged into chimeric recombinant adeno-associated viruses genotype 1/2 (rAAV1/2, Gene Detect) for high expression in mouse brain tissues. For direct stereotaxic injections of AAV into mouse striatum at 4 weeks of age, animals were first anesthetized by intraperitoneal injection of pentobarbital and placed on a stereotaxic apparatus. The stereotaxic injection coordinates used to deliver rAAV in the striatum were (in mm, with reference to bregma): anteroposterior, +0.5; mediolateral, ±1.5 and dorsoventral, −2.0 mm. Three microliters (equivalent to 4.5×10^9 genomic particles) of RFP-AAV1/2 and RFP-*asic1a* miR RNAi AAV1/2 was injected into the left and right striatum of the R6/2 mouse brain, respectively. Mice were sacrificed at 8 weeks of age and the amount of aggregation in the striatum was analyzed with a FTA.

Cell cultures and treatment

Mouse neuroblastoma cells (Neuro2a) and mouse embryonic fibroblasts (MEFs) were maintained in DMEM supplemented with 10% heat-inactivated FBS (Sigma), 2 mM L-glutamine and 100 U/ml penicillin/100 μg/ml streptomycin (Invitrogen) in a 5% CO_2 incubator at 37°C. Neuro2a cells were induced to express Nhtt-polyQ with 1 μM ponasterone A (Invitrogen) and differentiated to neuronal phenotype with 5 mM N^6,2′-*O*-dibutyryladenosine-3′,5′-cyclic monophosphate sodium salt (dbcAMP) (Nacalai tesque). MEFs were induced to Atg5$^{-/-}$ phenotype with 10 ng/ml doxycycline for 5 days as previously described (60). Neuro2a cells were incubated with either Ami or Ben at the time of differentiation and induction. For quantification of cell death, 5 μg/ml each of Hoechst 33342 (Molecular Probes) and propidium iodide (PI) were added to live cultures incubated with Ben. After 10 min at 37°C, the PI-positive cells were quantified with ArrayScan.

Generation of d2EGFP mice

A 6.0-kb *Hin*dIII fragment of rat genomic DNA (a kind gift of Dr Leonard Kaczmarek, Yale University) encompassing ≈5.3 kb regulatory sequences upstream of the transcription initiation site of the Kv3.1 gene followed by the first 739 bp of 5′ untranslated region was subcloned in the *Hin*dIII site of pEGFP-N1 (Clontech). This plasmid was linearized with *Eco*47III and *Afl*II, and the resulting ≈7 kb fragment was used to inject the pronuclei of fertilized eggs from C57Bl/6 × DBA F1 (BDF1) crosses. For details please refer to (38).

ArrayScan® quantification

For the quantification of aggregates, the number of RFP or ubi-dsRED cells, or the ubi-dsRED intensity, we employed the ArrayScan® VTI HCS Reader from Cellomics for high-throughput analysis. Protocols were designed according to the instruction manual. Before scanning, cells were first fixed with 3% paraformaldehyde in PBS for 1 h at 4°C and stained with 5 μg/ml Hoechst 33342 for 30 min. For quantifying the percentage of cells with aggregates, the first scan was to count the number of EGFP-positive spots in each field and the second one for the number of Hoechst-positive nuclei in the same fields. On the other hand, the quantification of RFP or ubi-dsRED cells could be accomplished with single scanning protocol. Scanning was performed in 24-well plates with duplicate or triplicate in each experimental condition. Each data point was generated from the quantification of at least 200 000 cells in each experimental set-up.

The *in vivo* study of Ben using R6/2 mice

To address the beneficial effect of Ben *in vivo*, we employed the R6/2 mouse model in which the progressive HD pathology is well characterized and has been extensively used for preclinical drug testing (5,61). HD mouse model R6/2 line containing 145 CAG repeats was originally purchased from The Jackson Laboratory. Mice that were selected for the *in vivo* studies carry CAG repeats from 120–130 (validated by Gene Scan). Water or Ben (5 or 1 mg/kg) was orally fed six times per week starting from 4 weeks of age (until the day they were sacrificed). Body weight was measured once per week. For the clasping testing, mice were suspended by the tail for 30 s and the clasping phenotype was graded to a particular level according to the following scale: 0, no clasping; 1, clasping of the forelimbs only; 2, clasping of both fore and hind limbs once or twice; 3, clasping of both fore and hind limbs more than three times or more than 5 s. For rota-rod testing, mice were initially placed on a rotating rod moving at 4 rpm and the speed was linearly increased up to 40 rpm in 300 s, and maintained at 40 rpm for 60 more seconds. Mice of 5 weeks to 12 weeks of age were all subjected to rota-rod testing with the same moving speed. For the survival

distribution, the number of days each mouse survived was recorded and the data collected for all the treatments (the mice that survived after 14 weeks and seizure-free; water, $n = 8$; tg-Ben1, $n = 10$ and tg-Ben5, $n = 9$) were subjected to Kaplan–Meier analysis followed by log-rank testing. All the experiments related to mouse were approved by the animal experiment committee of the RIKEN Brain Science Institute.

RNA interference

Each sense and anti-sense template with the hairpin backbone was synthesized (Operon) individually, annealed and ligated into the pSilencer 1.0 vector driven by a U6 promoter according to the instruction manual (Ambion). All plasmids containing shRNA inserts were sequence-verified. Plasmids containing shRNA inserts were transfected into Neuro2a cells with Lipofectamine 2000. Silencing was allowed to proceed for 2 days, total RNA was collected and semi-quantitative PCR was carried out as described. To show that the silencing effect occurred also at the protein level, we co-transfected expression vectors for each protein with its corresponding shRNA silencing vector. LacZ shRNA was used as a negative control for transfection. Supplementary Material, Fig. S6B shows the knockdown efficiency revealed by anti-V5 antibodies. The shRNA sequences can be found in the Supplementary method.

Chase experiment

To determine whether soluble Nhtt-polyQ degrades faster in the presence of Ben, we performed chase experiment. Inducible Neuro2a cells expressing Nhtt-60Q was chosen because the majority of the Nhtt-60Q remains soluble and only few aggregates can be observed. In brief, Neuro2a cells were first differentiated and induced to express Nhtt-60Q for 24 h. Ponasterone A was removed thereafter (dbcAMP was kept for maintaining the differentiation status) and cells were incubated with either water (control) or Ben of 50 μM (Day 0) for 4 days (Day 4). Fresh medium was replaced every 2 days with the same concentration of Ben, and cells were collected once per day until Day 4. Cells were subsequently lysed and the expression of soluble Nhtt-60Q was analyzed by western blotting with anti-huntingtin antibodies (the anti-em48).

Filter trap assay

FTA was performed with a Hybri-Dot manifold (BIO-RAD) and cellulose acetate membrane filter with pore size of 0.2 μm (Advantec). In brief, cells that were ready to be analyzed were lysed in the same lysis buffer used for western blotting, briefly sonicated and quantified with the BCA method as described. To prepare the brain for FTA, first we homogenized the whole brain 10 strokes at 1500 rpm with 1 ml homogenization buffer (50 mM Tris–HCl, pH 7.4, 150 mM NaCl, 1% Triton X-100, 1 mM PMSF and complete protease inhibitor cocktail) in a 5 cm^3 glass tube. Brain lysates were then briefly sonicated and the concentration was measured. Same amount of protein from each experimental condition was diluted to 100 μl with 2% SDS in PBS and applied onto the membrane. SDS-resistant aggregates stay while soluble proteins are removed by vacuum suction. Wells were washed twice with 2% SDS/PBS and vacuum suction was maintained for 20 min to allow complete and tight trapping of SDS insoluble aggregates. Membranes were subsequently blocked with 5% skim milk and immunoblot was performed.

Statistical analysis

We used unpaired student's *t*-test for comparison between two samples. One-way ANOVA Fisher's test followed by Tukey's HSD test was used for multiple comparisons with a 95% confidence level. For measuring the significance between different populations, we employed two-sample Kolmogorov–Smirnov test. For survival rate we plotted the survival distribution curve with the Kaplan–Meier method followed by log-rank testing (we generate all the data with XLSTAT software). We considered the difference between comparisons to be significant when $P < 0.05$ for all the statistical analysis.

SUPPLEMENTARY MATERIAL

Supplementary Material is available at *HMG* Online.

FUNDING

This work was supported by a Grant-in-Aid for Scientific Research on Priority Areas (Research on Pathomechanisms of Brain Disorders) from the Ministry of Education, Culture, Sports, Science and Technology of Japan (17025044) and by a Grant-in-Aid for the Research on Measures for Intractable Diseases from the Ministry of Health, Welfare and Labour, Japan.

ACKNOWLEDGEMENTS

We thank Professor Noboru Mizushima for the MEFs and anti-ATG5 antibodies; Dr Liakot A. Khan for discussion and technical assistance; Dr Joanna Doumanis for critical reading and discussion.

Conflict of Interest statement. None declared.

AUTHOR CONTRIBUTIONS

H.K.W. raised the hypothesis, tested the drug effects, performed most of the experiments, analyzed data, prepared figures and wrote the manuscript. P.O.B. and A.G. contributed to the experimental design, data analysis, discussion and critical commentary. M.K., C.W., M.Y. and Y.M. fed the mice and collected data for the *in vivo* studies of Ben in R6/2 mice. A.T. contributed to the construction of plasmids and DNA sequencing. T.K. generated the d2EGFP mouse line and contributed to critical discussion. T.N. contributed to some experiments for the data interpretation and discussion. N.N. supervised the project, contributed to discussion and critical reading of the manuscript.

REFERENCES

1. Cowan, C.M. and Raymond, L.A. (2006) Selective neuronal degeneration in Huntington's disease. *Curr. Top. Dev. Biol.*, **75**, 25–71.
2. The Huntington's Disease Collaborative Research Group (1993) A novel gene containing a trinucleotide repeat that is expanded and unstable on Huntington's disease chromosomes. *Cell*, **72**, 971–983.
3. Davies, S.W., Turmaine, M., Cozens, B.A., DiFiglia, M., Sharp, A.H., Ross, C.A., Scherzinger, E., Wanker, E.E., Mangiarini, L. and Bates, G.P. (1997) Formation of neuronal intranuclear inclusions underlies the neurological dysfunction in mice transgenic for the HD mutation. *Cell*, **90**, 537–548.
4. Arrasate, M., Mitra, S., Schweitzer, E.S., Segal, M.R. and Finkbeiner, S. (2004) Inclusion body formation reduces levels of mutant huntingtin and the risk of neuronal death. *Nature*, **431**, 805–810.
5. Li, J.Y., Popovic, N. and Brundin, P. (2005) The use of the R6 transgenic mouse models of Huntington's disease in attempts to develop novel therapeutic strategies. *NeuroRx*, **2**, 447–464.
6. Landles, C. and Bates, G.P. (2004) Huntingtin and the molecular pathogenesis of Huntington's disease. Fourth in molecular medicine review series. *EMBO Rep.*, **5**, 958–963.
7. Browne, S.E. and Beal, M.F. (2004) The energetics of Huntington's disease. *Neurochem. Res.*, **29**, 531–546.
8. Harms, L., Meierkord, H., Timm, G., Pfeiffer, L. and Ludolph, A.C. (1997) Decreased *N*-acetyl-aspartate/choline ratio and increased lactate in the frontal lobe of patients with Huntington's disease: a proton magnetic resonance spectroscopy study. *J. Neurol. Neurosurg. Psychiatry*, **62**, 27–30.
9. Jenkins, B.G., Koroshetz, W.J., Beal, M.F. and Rosen, B.R. (1993) Evidence for impairment of energy metabolism in vivo in Huntington's disease using localized 1H NMR spectroscopy. *Neurology*, **43**, 2689–2695.
10. Jenkins, B.G., Rosas, H.D., Chen, Y.C., Makabe, T., Myers, R., MacDonald, M., Rosen, B.R., Beal, M.F. and Koroshetz, W.J. (1998) 1H NMR spectroscopy studies of Huntington's disease: correlations with CAG repeat numbers. *Neurology*, **50**, 1357–1365.
11. Reynolds, N.C., Jr, Prost, R.W. and Mark, L.P. (2005) Heterogeneity in 1H-MRS profiles of presymptomatic and early manifest Huntington's disease. *Brain Res.*, **1031**, 82–89.
12. Tsang, T.M., Woodman, B., McLoughlin, G.A., Griffin, J.L., Tabrizi, S.J., Bates, G.P. and Holmes, E. (2006) Metabolic characterization of the R6/2 transgenic mouse model of Huntington's disease by high-resolution MAS 1H NMR spectroscopy. *J. Proteome Res.*, **5**, 483–492.
13. Tkac, I., Dubinsky, J.M., Keene, C.D., Gruetter, R. and Low, W.C. (2007) Neurochemical changes in Huntington R6/2 mouse striatum detected by in vivoH NMR spectroscopy. *J. Neurochem*, **100**, 1397–1406.
14. Walz, W. and Mukerji, S. (1988) Lactate release from cultured astrocytes and neurons: a comparison. *Glia*, **1**, 366–370.
15. Yao, H. and Haddad, G.G. (2004) Calcium and pH homeostasis in neurons during hypoxia and ischemia. *Cell Calcium*, **36**, 247–255.
16. Xiong, Z.G., Zhu, X.M., Chu, X.P., Minami, M., Hey, J., Wei, W.L., MacDonald, J.F., Wemmie, J.A., Price, M.P., Welsh, M.J. *et al.* (2004) Neuroprotection in ischemia: blocking calcium-permeable acid-sensing ion channels. *Cell*, **118**, 687–698.
17. Yermolaieva, O., Leonard, A.S., Schnizler, M.K., Abboud, F.M. and Welsh, M.J. (2004) Extracellular acidosis increases neuronal cell calcium by activating acid-sensing ion channel 1a. *Proc. Natl. Acad. Sci. USA*, **101**, 6752–6757.
18. Atwood, C.S., Moir, R.D., Huang, X., Scarpa, R.C., Bacarra, N.M., Romano, D.M., Hartshorn, M.A., Tanzi, R.E. and Bush, A.I. (1998) Dramatic aggregation of Alzheimer abeta by Cu(II) is induced by conditions representing physiological acidosis. *J. Biol. Chem.*, **273**, 12817–12826.
19. Waldmann, R., Champigny, G., Bassilana, F., Heurteaux, C. and Lazdunski, M. (1997) A proton-gated cation channel involved in acid-sensing. *Nature*, **386**, 173–177.
20. Alvarez de la Rosa, D., Krueger, S.R., Kolar, A., Shao, D., Fitzsimonds, R.M. and Canessa, C.M. (2003) Distribution, subcellular localization and ontogeny of ASIC1 in the mammalian central nervous system. *J. Physiol.*, **546**, 77–87.
21. Krishtal, O. (2003) The ASICs: signaling molecules? Modulators? *Trends Neurosci.*, **26**, 477–483.
22. Wemmie, J.A., Price, M.P. and Welsh, M.J. (2006) Acid-sensing ion channels: advances, questions and therapeutic opportunities. *Trends Neurosci.*, **29**, 578–586.
23. Wemmie, J.A., Askwith, C.C., Lamani, E., Cassell, M.D., Freeman, J.H., Jr and Welsh, M.J. (2003) Acid-sensing ion channel 1 is localized in brain regions with high synaptic density and contributes to fear conditioning. *J. Neurosci.*, **23**, 5496–5502.
24. Wemmie, J.A., Chen, J., Askwith, C.C., Hruska-Hageman, A.M., Price, M.P., Nolan, B.C., Yoder, P.G., Lamani, E., Hoshi, T., Freeman, J.H., Jr *et al.* (2002) The acid-activated ion channel ASIC contributes to synaptic plasticity, learning, and memory. *Neuron*, **34**, 463–477.
25. Wu, L.J., Duan, B., Mei, Y.D., Gao, J., Chen, J.G., Zhuo, M., Xu, L., Wu, M. and Xu, T.L. (2004) Characterization of acid-sensing ion channels in dorsal horn neurons of rat spinal cord. *J. Biol. Chem.*, **279**, 43716–43724.
26. Ugawa, S., Ueda, T., Ishida, Y., Nishigaki, M., Shibata, Y. and Shimada, S. (2002) Amiloride-blockable acid-sensing ion channels are leading acid sensors expressed in human nociceptors. *J. Clin. Invest.*, **110**, 1185–1190.
27. Voilley, N., de Weille, J., Mamet, J. and Lazdunski, M. (2001) Nonsteroid anti-inflammatory drugs inhibit both the activity and the inflammation-induced expression of acid-sensing ion channels in nociceptors. *J. Neurosci.*, **21**, 8026–8033.
28. Gao, J., Duan, B., Wang, D.G., Deng, X.H., Zhang, G.Y., Xu, L. and Xu, T.L. (2005) Coupling between NMDA receptor and acid-sensing ion channel contributes to ischemic neuronal death. *Neuron*, **48**, 635–646.
29. Cragoe, E.J., Jr, Woltersdorf, O.W., Jr, Bicking, J.B., Kwong, S.F. and Jones, J.H. (1967) Pyrazine diuretics. II. N-amidino-3-amino-5-substituted 6-halopyrazinecarboxamides. *J. Med. Chem.*, **10**, 66–75.
30. Kleyman, T.R. and Cragoe, E.J., Jr (1988) Amiloride and its analogs as tools in the study of ion transport. *J. Membr. Biol.*, **105**, 1–21.
31. Cuthbert, A.W. and Edwardson, J.M. (1979) Synthesis, properties and biological activity of tritiated *N*-benzylamidino-3,5-diamino-6-chloro-pyrazine carboxamide—a new ligand for epithelial sodium channels. *J. Pharm. Pharmacol.*, **31**, 382–386.
32. Kotliarova, S., Jana, N.R., Sakamoto, N., Kurosawa, M., Miyazaki, H., Nekooki, M., Doi, H., Machida, Y., Wong, H.K., Suzuki, T. *et al.* (2005) Decreased expression of hypothalamic neuropeptides in Huntington disease transgenic mice with expanded polyglutamine-EGFP fluorescent aggregates. *J. Neurochem.*, **93**, 641–653.
33. Wang, G.H., Mitsui, K., Kotliarova, S., Yamashita, A., Nagao, Y., Tokuhiro, S., Iwatsubo, T., Kanazawa, I. and Nukina, N. (1999) Caspase activation during apoptotic cell death induced by expanded polyglutamine in N2a cells. *Neuroreport*, **10**, 2435–2438.
34. Benson, C.J., Xie, J., Wemmie, J.A., Price, M.P., Henss, J.M., Welsh, M.J. and Snyder, P.M. (2002) Heteromultimers of DEG/ENaC subunits form H^+-gated channels in mouse sensory neurons. *Proc. Natl. Acad. Sci. USA*, **99**, 2338–2343.
35. Khan, L.A., Bauer, P.O., Miyazaki, H., Lindenberg, K.S., Landwehrmeyer, B.G. and Nukina, N. (2006) Expanded polyglutamines impair synaptic transmission and ubiquitin-proteasome system in *Caenorhabditis elegans*. *J. Neurochem.*, **98**, 576–587.
36. Machida, Y., Okada, T., Kurosawa, M., Oyama, F., Ozawa, K. and Nukina, N. (2006) rAAV-mediated shRNA ameliorated neuropathology in Huntington disease model mouse. *Biochem. Biophys. Res. Commun.*, **343**, 190–197.
37. Andreatta, C., Nahreini, P., Hovland, A.R., Kumar, B., Edwards-Prasad, J. and Prasad, K.N. (2001) Use of short-lived green fluorescent protein for the detection of proteasome inhibition. *Biotechniques*, **30**, 656–660.
38. Metzger, F., Repunte-Canonigo, V., Matsushita, S., Akemann, W., Diez-Garcia, J., Ho, C.S., Iwasato, T., Grandes, P., Itohara, S., Joho, R.H. *et al.* (2002) Transgenic mice expressing a pH and Cl- sensing yellow-fluorescent protein under the control of a potassium channel promoter. *Eur. J. Neurosci.*, **15**, 40–50.
39. Hauck, B., Chen, L. and Xiao, W. (2003) Generation and characterization of chimeric recombinant AAV vectors. *Mol. Ther.*, **7**, 419–425.
40. Friese, M.A., Craner, M.J., Etzensperger, R., Vergo, S., Wemmie, J.A., Welsh, M.J., Vincent, A. and Fugger, L. (2007) Acid-sensing ion channel-1 contributes to axonal degeneration in autoimmune inflammation of the central nervous system. *Nat. Med.*, **13**, 1483–1489.
41. Kiedrowski, L. (2007) NCX and NCKX operation in ischemic neurons. *Ann. N. Y. Acad. Sci.*, **1099**, 383–395.
42. Realini, C. and Rechsteiner, M. (1995) A proteasome activator subunit binds calcium. *J. Biol. Chem.*, **270**, 29664–29667.

43. Kawahara, H. and Yokosawa, H. (1994) Intracellular calcium mobilization regulates the activity of 26 S proteasome during the metaphase-anaphase transition in the ascidian meiotic cell cycle. *Dev. Biol.*, **166**, 623–633.
44. Uvarov, A.V. and Mesaeli, N. (2008) Enhanced ubiquitin-proteasome activity in calreticulin deficient cells: A compensatory mechanism for cell survival. *Biochim. Biophys. Acta.*, **1783**, 1237–1247.
45. Chiba, K., Alderton, J.M., Hoshi, M. and Steinhardt, R.A. (1999) Activation of the proteasomes of sand dollar eggs at fertilization depends on the intracellular pH rise. *Dev. Biol.*, **209**, 52–59.
46. Asai, A., Tanahashi, N., Qiu, J.H., Saito, N., Chi, S., Kawahara, N., Tanaka, K. and Kirino, T. (2002) Selective proteasomal dysfunction in the hippocampal CA1 region after transient forebrain ischemia. *J. Cereb. Blood Flow Metab.*, **22**, 705–710.
47. Keller, J.N., Huang, F.F., Zhu, H., Yu, J., Ho, Y.S. and Kindy, T.S. (2000) Oxidative stress-associated impairment of proteasome activity during ischemia-reperfusion injury. *J Cereb. Blood Flow Metab.*, **20**, 1467–1473.
48. Reinstein, E. and Ciechanover, A. (2006) Narrative review: protein degradation and human diseases: the ubiquitin connection. *Ann. Intern. Med.*, **145**, 676–684.
49. Ross, C.A. and Pickart, C.M. (2004) The ubiquitin-proteasome pathway in Parkinson's disease and other neurodegenerative diseases. *Trends Cell Biol.*, **14**, 703–711.
50. Jana, N.R., Zemskov, E.A., Wang, G. and Nukina, N. (2001) Altered proteasomal function due to the expression of polyglutamine-expanded truncated N-terminal huntingtin induces apoptosis by caspase activation through mitochondrial cytochrome c release. *Hum. Mol. Genet.*, **10**, 1049–1059.
51. Bence, N.F., Sampat, R.M. and Kopito, R.R. (2001) Impairment of the ubiquitin-proteasome system by protein aggregation. *Science*, **292**, 1552–1555.
52. Bennett, E.J., Bence, N.F., Jayakumar, R. and Kopito, R.R. (2005) Global impairment of the ubiquitin-proteasome system by nuclear or cytoplasmic protein aggregates precedes inclusion body formation. *Mol. Cell*, **17**, 351–365.
53. Bennett, E.J., Shaler, T.A., Woodman, B., Ryu, K.Y., Zaitseva, T.S., Becker, C.H., Bates, G.P., Schulman, H. and Kopito, R.R. (2007) Global changes to the ubiquitin system in Huntington's disease. *Nature*, **448**, 704–708.
54. Taguchi, N., Niisato, N., Sawabe, Y., Miyazaki, H., Hirai, Y. and Marunaka, Y. (2005) Benzamil, a blocker of epithelial Na(+) channel-induced upregulation of artery oxygen pressure level in acute lung injury rabbit ventilated with high frequency oscillation. *Biochem. Biophys. Res. Commun.*, **327**, 915–919.
55. Huang, B.S. and Leenen, F.H. (2005) Blockade of brain mineralocorticoid receptors or Na+ channels prevents sympathetic hyperactivity and improves cardiac function in rats post-MI. *Am. J. Physiol. Heart Circ. Physiol.*, **288**, H2491–H2497.
56. Sagnella, G.A. and Swift, P.A. (2006) The renal epithelial sodium channel: genetic heterogeneity and implications for the treatment of high blood pressure. *Curr. Pharm. Des.*, **12**, 2221–2234.
57. Kleyman, T.R. and Cragoe, E.J., Jr (1990) Cation transport probes: the amiloride series. *Methods Enzymol.*, **191**, 739–755.
58. Xiong, Z.G., Pignataro, G., Li, M., Chang, S.Y. and Simon, R.P. (2007) Acid-sensing ion channels (ASICs) as pharmacological targets for neurodegenerative diseases. *Curr. Opin. Pharmacol*, **8**, 25–32.
59. Mizushima, N., Yamamoto, A., Hatano, M., Kobayashi, Y., Kabeya, Y., Suzuki, K., Tokuhisa, T., Ohsumi, Y. and Yoshimori, T. (2001) Dissection of autophagosome formation using Apg5-deficient mouse embryonic stem cells. *J. Cell. Biol.*, **152**, 657–668.
60. Hosokawa, N., Hara, Y. and Mizushima, N. (2006) Generation of cell lines with tetracycline-regulated autophagy and a role for autophagy in controlling cell size. *FEBS Lett.*, **580**, 2623–2629.
61. Mangiarini, L., Sathasivam, K., Seller, M., Cozens, B., Harper, A., Hetherington, C., Lawton, M., Trottier, Y., Lehrach, H., Davies, S.W. *et al.* (1996) Exon 1 of the HD gene with an expanded CAG repeat is sufficient to cause a progressive neurological phenotype in transgenic mice. *Cell*, **87**, 493–506.